

PACS numbers: 42.55.Vc; 52.38.Ph
DOI: 10.1070/QE2001v031n08ABEH002027

Theoretical investigation of a Ni-like xenon X-ray laser in the 13 – 14 nm range

E P Ivanova, N A Zinov'ev, L V Knight

***Abstract*. Several efficient laser transitions in Ni-like xenon in the 13 – 14-nm range are predicted on the basis of atomic kinetic calculations of the gains. The time characteristics of the gain $g(\tau)$ as functions of the electron density, temperature, and the diameter of the plasma column are considered. The results of calculations can be used to optimise the pump parameters with the aim of maximising the gain.**

Keywords: *simulation of X-ray lasers, atomic kinetic calculation, Ni-like xenon.*

1. Introduction

At present, the feasibility of VUV lasing in the 13 – 14 nm range is actively investigated, because it is for this wavelength range that the techniques of producing multilayer mirrors with reflectivities about 60 % have been elaborated [1 – 3]. The laser radiation in this spectral region is employed in microlithography, X-ray microscopy, biotechnology, etc.

In recent years, new experimental approaches were introduced to develop efficient VUV lasers. In particular, an investigation was made of intense 1 – 22-nm radiation from a gas puff target pumped by 0.9 – 10-ns Nd : YAG-laser pulses with an energy of ~ 0.7 J [4]. A 'light spark plasma source' of this type was elaborated even in the early 1970s [5]. As of now, it is one of the promising devices for the production of non-compressed unablative plasma with the aim to obtain lasing in the 1 – 5-nm range [6]. A hybrid pump source was elaborated in Ref. [7]: an electric capillary discharge produces a low-temperature plasma in the state of Ne-like sulphur and a picosecond pump laser subsequently heats the plasma. Temperatures of the order of several hundred electronvolts can be obtained in these non-pinching plasma sources.

The collisional-radiative model describing the occurrence of amplification of spontaneous emission (ASE) on Ni-like ion transitions is similar to that in Ne-like ions proposed in the early 1970s [8 – 10]. The first experimental observations of the ASE with Ni-like ions [11] demonstrated the economy of the Ni-like scheme as compared with the Ne-like one, for the ratio of the laser transition energy in a Ni-like ion to its production energy is significantly lower than in a Ne-like ion. In the first investigations involving Ni-like ions, advantage was taken of a single long laser pump pulse (0.5 – 1.5 ns) [11, 12]. The outcome of these investigations was a significant advancement to the far VUV spectral region and to the water window range ($\lambda < 44$ Å). However, the gains and the brightness of an output laser beam from a Ni-like ion plasma proved to be substantially lower than in lasers on Ne-like ions. In subsequent investigations, two- and multistep configurations of laser-assisted pumping of plasma were used to improve the efficiency of Ni-like schemes [13 – 15].

The advantages of multistep pumping are evident: in the course of a prepulse, there occurs plasma ionisation and expansion, and the plasma density gradient flattens during the interpulse interval. Thus, there forms a relatively uniform plasma region with a density required for the occurrence of lasing. By the time of arrival of the main pulse, the working ionisation stage should be reached. The main pulse next heats the plasma, bringing it to the inverted state. Therefore, a multistep pumping provides better conditions for the propagation of a laser beam by passing it through a more uniform medium, optimises the ionisation balance, and significantly raises the electron-to-ion temperature ratio T_e/T_i, resulting in an increase in gain coefficients. Nevertheless, the quantum laser yield reported in Refs [13 – 15] was no greater than 10^{-6}.

In many experiments, the small plasma length L was due to the short duration of the output laser pulse ($\tau_{las} < 100$ ps), which is related to the short inversion lifetime in the plasma with the optimal electron density n_e and temperature T_e. The aim of our investigations is the generation of short and ultrashort VUV laser pulses. For several applications, however, it is important to maximise the plasma column gain – length product gL. Increasing L has become possible with the use of travelling-wave excitation (TWE) technique [2, 3]: a laser pump beam is scanned along the sample leading the propagation of the output laser radiation. The use of TWE in Ref. [2] allowed attaining $gL > 30$ for the $3d4d - 3d4p$ (0 – 1) Ni-like silver transition with $\lambda = 139$ Å.

The pump sources are optimised to attain the parameters n_e^{opt} and T_e^{opt} that maximise $g(\tau)$; in this case, it is especially significant to take into account the time characteristics of the processes occurring in a plasma. For two- and multistep schemes, at least three time characteristics should be emphasised: the time interval $\tau_0(n_e, T_e)$ for the attainment of the

E P Ivanova, N A Zinov'ev Institute of Spectroscopy, Russian Academy of Sciences, 142190 Troitsk, Moscow oblast, Russia;
L V Knight Brigham Young University, Provo, UT 84602, USA

Received 14 March 2001
Kvantovaya Elektronika **31** (8) 683 – 688 (2001)
Translated by E N Ragozin

working ionisation stage (the Ni-like xenon stage in our case) in the plasma heating; the population time of Ni-like ion levels $\tau_{ex}(n_e, T_e, d)$ (d is the diameter of the plasma column); and the time of Ni-like ion ionisation to the next (Co-like) stage $\tau_i^{Ni}(n_e, T_e)$, i.e., the Ni-like ion lifetime in the plasma. In many experiments, the VUV-laser saturation length is caused by either the lifetime $\tau_i^{Ni}(n_e, T_e)$, or the time interval $\tau_{ex}(n_e, T_e, d)$.

In Refs [16, 17], we calculated the gains on the transitions of ions of the neon isoelectronic sequence. We found that inversion between highly excited states of Ne-like ions is possible for specific plasma parameters. In particular, $2s2p^6 3d\,[J = 2] - 2s2p^6 3p\,[J = 1]$ are strong laser transitions in Ne-like ions, i.e., the $3d - 3p(2 - 1)$ transition, in which 'an observer' is the $2s$ vacancy of the core. The laser transitions between highly excited states lie in the spectral region with a high line density, which hinders their spectroscopic identification. The data on experimental measurements of the gains on the $3d - 3p(2 - 1)$ transition in Ne-like germanium are nevertheless reported in the literature [18]. Similar laser transitions between highly excited states of Ni-like tantalum were theoretically investigated in Ref. [19]. The calculations suggest that a significant expansion of the laser transition wavelength range is possible for every ion. However, the laser transitions between excited levels remain unexplored for the overwhelming majority of ions.

The VUV laser investigations involving Ni-like xenon have not been reported in the literature. At present, the search for lasing in this system is actively pursued employing gas–puff devices, where the plasma is produced by a two-step pump laser irradiation [4, 6]. Theoretical calculations of the gains indicating the optimal plasma parameters and the time characteristics $\tau_0(n_e, T_e)$, $\tau_{ex}(n_e, T_e, d)$, and $\tau_i^{Ni}(n_e, T_e)$ may prove to be of utility. Here, we carry out a comprehensive investigation of the gain $g(\tau; n_e, T_e, d)$ for all possible laser transitions in Ni-like xenon, including the strong laser lines in the 13–14-nm range. It is assumed that the capillary plasma is produced by a two-step pump pulse similar to that employed in Refs [4, 6]. We calculate the time characteristics as well as n_e, T_e, and d.

2. Calculation of the gains for Ni-like xenon transitions

X-ray laser simulations can be divided into three interrelated stages: magnetohydrodynamic (MHD) calculations of plasma heating and plasma dynamics; atomic kinetic calculations of level populations, line intensities, and gains; and calculations of radiation propagation through the plasma, with estimates of saturation lengths and coherence. Each stage is an intricate problem involving a large parameter set. Since laser amplification is observable in a strictly defined range of plasma parameters, atomic kinetic calculations of the gains become vitally important. They allow determining the plasma parameters optimised for maximum laser effect on each of the possible transitions. In our calculations we assume MHD calculations and the kinetics of ion level population to be independent problems in the first approximation, because the plasma dynamics is hardly affected by the electron excitation and the radiative decay of an individual ion.

Here, we do not enlarge on the method of gain calculations, which was outlined in detail elsewhere [16, 20]. In the context of a collisional-radiative model, laser transitions are possible between the states of neon, nickel, and palladium ion isoelectronic sequences. For all known laser transitions in these ions, $\Delta n = 0$ (n is the principal quantum number of a state). By the example of $2p^5 3p[J = 0] - 2p^5 3s[J = 1]$ and $2p^5 3p[J = 2] - 2p^5 3s[J = 1]$ transitions in Ne-like germanium, a full calculation of line broadening taking into account the Stark effect, which arises due to quasistatic plasma microfields, was made in Ref. [21].

The calculation showed that the line broadening caused by quasistatic ion microfields is negligible in this case. The laser effect is maximum for rather high T_e and n_e. In Ni-like xenon, in particular, the conditions $T_e \geqslant 500$ eV and $n_e \geqslant 10^{20}$ cm^{-3} should be fulfilled. In this case, the Doppler and intrinsic line widths are of the order of hundreds of inverse centimetres. This far exceeds the splittings of fine and hyperfine structures caused by quasistatic ion microfields. The line broadening due to collisions with electrons is several times greater than the Doppler broadening. For the above reasons, the contribution to the broadening made by quasistatic microfields was neglected in the calculation of the line widths.

Because the collisional mixing is so strong, the upper (P_{up}) and lower (P_{low}) level populations are close, so that the inversion $P_{up} - P_{low}(g_{up}/g_{low})$ is ordinarily equal to 10–30 % of the upper level population (g_{up}, g_{low} are the degeneracy coefficients of the upper and lower levels). Therefore, the collisional and radiative transition rates for the working ion should be calculated with a high precision to adequately describe the physical processes in the plasma. In this case, it is significant that all transition rates be calculated in one and the same approximation.

In our model, a consistent quantum-electrodynamic theory underlies the calculations of energy levels, radiative transition probabilities (RTPs), and ion excitation cross sections by electron impact. The method of atomic calculations in use is referred to as the relativistic perturbation theory with a zero-approximation model potential. This method is described elsewhere [22–24]. Also given in these papers is a comprehensive analysis of the spectroscopic constants and a comparison with the calculations made by other authors.

Table 1 gives the classification in the jj-coupling scheme and the brief designations for the transitions under study which can exhibit ASE for specific plasma parameters. Also given are their wavelengths and the RTPs. For brevity, transitions are denoted by the order numbers of the levels (in the order of increasing energy). The first two transitions in Table 1 have been most studied in the nickel isoelectronic sequence. As regards the inversion mechanism, the $3d4d - 3d4p(0 - 1)$ transition is similar to the $2p3p - 2p3s(0 - 1)$ transition in a Ne-like ion. The inversion on the $3d4f - 3d4d(1 - 1)$ transition is caused by the reabsorption to the upper level, the high rate of electron collisional population of this level from the ground state, and also by the relatively high RTP from the upper state to the lower one.

In an optically thin medium, the upper resonance $3d_{3/2}4f_{5/2}[J = 1]$ level decays to the ground state with a probability of 6×10^{13} s^{-1}. In an optically dense medium, the reabsorption lowers the probability of this decay by a factor of 10–100, with the result that the population of the upper $3d_{3/2}4f_{5/2}[J = 1]$ state is significantly increased, which explains the occurrence of inversion. Characteristically, the inversion lifetime for this transition, as well as for the inner-shell $3p - 3d(0 - 1)$ transitions with $\lambda = 45$, 39.1, and 39.9 Å

Table 1. States of Ni-like xenon which can give rise to transitions exhibiting amplification of spontaneous emission, transition wavelengths λ, and corresponding RTPs.

Upper state		Lower state		Transition	λ/Å	RTP/s^{-1}
Level	J	Level	J			
$3d_{5/2}4d_{5/2}$	0	$3d_{5/2}4p_{3/2}$	1	35–12	99.0	1.0×10^{11}
$3d_{3/2}4f_{5/2}$	1	$3d_{3/2}4d_{1/2}$	1	57–28	113	4.4×10^{10}
$3p_{3/2}4p_{3/2}$	0	$3d_{3/2}4p_{1/2}$	1	65–9	45.0	1.68×10^{11}
$3p_{1/2}4p_{1/2}$	0	$3p_{1/2}4s_{1/2}$	1	67–61	197	1.9×10^{10}
$3p_{1/2}4p_{1/2}$	0	$3d_{3/2}4p_{1/2}$	1	67–9	39.1	8.9×10^{11}
$3p_{1/2}4p_{1/2}$	0	$3d_{5/2}4p_{3/2}$	1	67–12	39.9	2.2×10^{11}
$3p_{1/2}4p_{3/2}$	2	$3p_{1/2}4s_{1/2}$	1	69–61	173	5.0×10^{10}
$3p_{3/2}4d_{5/2}$	4	$3p_{3/2}4p_{3/2}$	3	74–62	143	1.2×10^{11}
$3p_{1/2}4d_{3/2}$	2	$3p_{1/2}4p_{1/2}$	1	78–66	118	1.6×10^{11}
$3p_{1/2}4d_{5/2}$	2	$3p_{1/2}4p_{3/2}$	1	80–68	138.6	1.1×10^{11}
$3p_{1/2}4d_{5/2}$	3	$3p_{3/2}4p_{5/2}$	2	81–69	139.0	1.2×10^{11}
$3p_{3/2}4f_{7/2}$	2	$3p_{3/2}4d_{5/2}$	1	89–76	132	9.6×10^{10}
$3p_{1/2}4f_{5/2}$	2	$3p_{1/2}4d_{3/2}$	1	93–79	130	1.1×10^{11}

of Ni-like xenon, is 10–20 ps, hindering their observation with conventional approaches. The laser transitions in the 130–140 Å wavelength range (the lower four lines in Table 1) are most efficient.

In the calculation of parameters of the pump pulses, an important part is played by the temporal factors mentioned in the Introduction. Our model allows an estimate of the plasma ionisation balance with inclusion of two ionisation stages – the Cu- and Ni-like ones – and also the time characteristics: the ionisation time for a Cu-like ion $\tau_i^{Cu}(n_e, T_e)$, τ_{ex}, and τ_i^{Ni} [20]. Table 2 gives the ionisation balance in the xenon plasma as well as the Cu-to-Ni-like ion ionisation time as functions of the plasma parameters n_e and T_e. Referring to Table 2, relatively small changes of the plasma parameters may be responsible for a significant variation of ionisation time. The data collected in Table 2 allow the estimate of the ionisation balance and the time of ionisation of the Ni-like ion to the Cu-like one. For $T_e = 500 - 600$ eV, the Ni-like ion is in a 'thermal trap', i.e., the ionisation and the recombination to the Ni-like ion are practically balanced.

Fig. 1 shows the gains for the strongest laser transitions as functions of n_e for $T_e = 600$ eV and $d = 100$ μm. For the conventional $4d - 4p(0-1)$ transition with $\lambda = 99$ Å, the optimal density $n_e^{opt} = 10^{20}$ cm^{-3}. For other transitions, n_e^{opt} is higher. For instance, $n_{opt} \geqslant 5\times10^{20}$ cm^{-3} for the $4f-4d(2-1)$ transition with $\lambda = 130$ Å. Fig. 2a shows the dependences of the gain g on time for the $4d - 4p(0-1)$ transition assuming an instantaneous plasma heating by the main pump pulse. When calculating $g(\tau)$ we assume only the ground state of Ni-like ions to be populated at the point in time $\tau = 0$. In this case, a correction coefficient is used to take into account that a fraction of ions are in other ionisation stages.

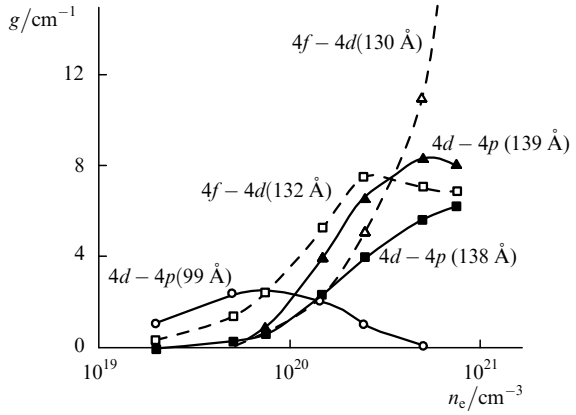

Figure 1. Time-averaged gains g as functions of n_e for the strongest transitions in Ni-like xenon for $T_e = 600$ eV, $d = 0.1$ mm.

The curves in Fig. 2a corresponding to different T_e have a sharp asymmetric peak for $\tau = 1 - 2$ ps; subsequently, the function $g(\tau)$ smoothly approaches the asymptotic value. With increase in T_e, the peak gain increases. In this case, its asymptotic value lowers. The decrease of the asymptotic values of $g(\tau)$ is caused by a reduction of the number of Ni-like ions due to ionisation to the Co-like state. Therefore, $g(\tau)$ averaged over an interval of 600 ps peaks for $T_e = 600$ eV. For $T_e > 600$ eV, the function $g_{max}(\tau) \simeq 16-18$ cm^{-1} for $\tau = 1 - 2$ ps and decays for $\tau \sim 10 - 15$ ps. This sharp peak is due to a large difference in electron collisional rates of population from the ground state between the upper ($3d4d[J=0]$) and lower ($3d4p[J=1]$) working levels. During the time period corresponding to this peak, the effect of collisional mixing with the remaining levels is still small. This inversion mechanism was termed 'transient' in Ref. [25]. After peaking, the population densities and the inversions approach their quasistationary values determined by collisional mixing with other levels.

Fig. 2b gives functions $g(\tau)$ for the $4f - 4d(2-1)$ transition with $\lambda = 130$ Å; here, $g(\tau)$ averaged over the 0–600 ps

Table 2. Ionisation balance in the xenon plasma taking into account the Ni- and Cu-like stages of ionisation as a function of the plasma parameters n_e and T_e ([Ni] denotes the fraction of Ni-like ions, [Ni] + [Cu] = 1, and τ_i^{Cu} denotes the Cu-to-Ni-like stage ionisation time; $k = T_e/E_{ionis}$, where E_{ionis} is the ionisation energy for a Cu-like ion).

$n_e/10^{19}$ cm^{-3} ⟶		5		7.5		10		25		50		100	
T_e/eV	k	[Ni]	τ_i^{Cu}/ns	[Ni]	τ_i^{Cu}/ns	[Ni]	τ_i^{Cu}/ns	[Ni]	τ_i^{Cu}/ns	[Ni]	τ_i^{Cu}/ns	[Ni]	τ_i^{Cu}/ns
200	0.23	0.18	4.2	0.19	3.2	0.20	1.6	0.23	0.75	0.25	0.3	0.25	0.15
250	0.29	0.36	2.9	0.36	1.6	0.37	0.8	0.42	0.3	0.44	0.15	0.47	0.06
300	0.35	0.52	1.9	0.54	0.8	0.55	0.4	0.60	0.14	0.63	0.06	0.67	0.05
350	0.41	0.63	1.0	0.65	0.3	0.68	0.2	0.72	0.07	0.74	0.03	0.76	0.03
400	0.47	0.71	0.5	0.73	0.15	0.75	0.1	0.78	0.04	0.82	0.02	0.82	0.015
450	0.51	0.80	0.1	0.81	0.07	0.82	0.05	0.84	0.03	0.86	0.015	0.86	0.01

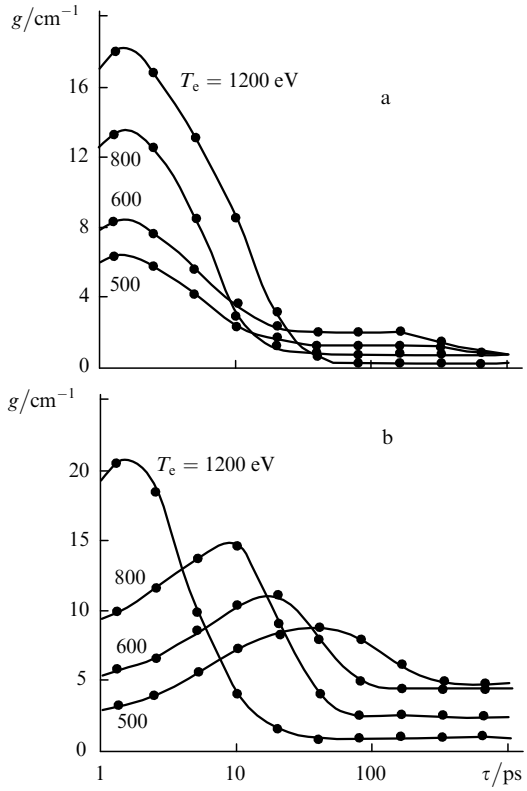

Figure 2. Time dependences $g(\tau)$ for the $4d-4p(0-1)$ [$\lambda = 99$ Å (a)] and $4f-4d(2-1)$ [$\lambda = 130$ Å (b)] transitions for a two-step pumping and plasma parameters $n_e = 1.5 \times 10^{20}$ (a), 5×10^{20} cm^{-3} (b), $d =$ 0.1 mm and different T_e.

interval peaks for $T_e = 600$ eV. Higher T_e result in higher values of $g_{max}(\tau)$, whereas its asymptotic value lowers due to reduction of the Ni-like fraction.

We also considered the time dependences in the case of a single long pump pulse. Here, the calculation was made assuming that the lower level of a Cu-like ion is initially populated, i.e. that the production of a Ni-like ion and its excitation take place under pump pulse irradiation. In this case, the ionisation balance is far from being optimal, the duration of the inverted state and $g(\tau)$ are smaller, and $n_e^{opt} \approx 5 \times 10^{20}$ cm^{-3} for all transitions.

For several transitions given in Table 1, Fig. 3 shows the $g(\tau)$ functions for n_e^{opt} and $T_e = 400$ eV – the minimal temperature whereby amplification is possible. In real experiments, the intensities should be measured in a short time interval, which is hard to accomplish. Proceeding from the calculated value of the ionisation time $\tau_i^{Cu}(n_e, T_e)$ (Table 2), it is possible to make a coarse estimate of the pump pulse duration $\tau_0(n_e, T_e)$ required to reach the Ni-like stage in relation to the relevant parameters of the non-compressed uncontaminated plasma. The pulse duration depends only slightly on its shape; we believe that $\tau_0(n_e, T_e)$ is approximately two orders of magnitude longer than the $\tau_i^{Cu}(n_e, T_e)$ times specified in Table 2.

Of particular interest is the little-studied $4f-4d(1-1)$ transition with $\lambda = 113$ Å whose inversion mechanism is due to reabsorption (the second line in Table 1). The ASE on this transition was experimentally investigated in Ni-like ions of molybdenum [26] and silver [2]. In the context of a two-step pumping with recourse to TWE, $g = 30-33$ cm^{-1} for this transition for $T_e \sim 800$ eV [2]. In Ni-like xenon,

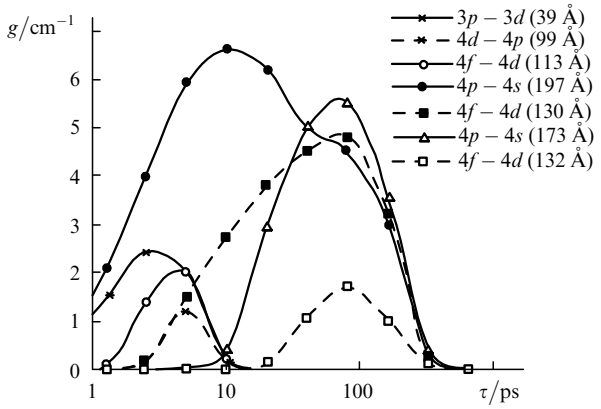

Figure 3. Time dependences $g(\tau)$ for several Ni-like xenon transitions in the case of a single pump pulse for the plasma parameters $n_e = 5 \times 10^{20}$ cm^{-3}, $d = 0.1$ mm, and $T_e = 400$ eV.

$g_{max}(\tau) = 1$ cm^{-1} for a single pump pulse and optimal plasma parameters (Fig. 3). Fig. 4 depicts the $g(\tau)$ dependence in the case of a two-step pump for n_e^{opt}, T_e^{opt}, where $g_{max}(\tau) > 25$ cm^{-1}.

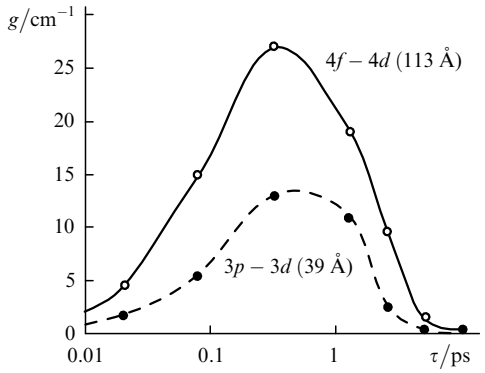

Figure 4. Time dependences $g(\tau)$ for the $4f-4d(1-1)$ transition ($\lambda =$ 113 Å) with reabsorption and for the $3p-3d(0-1)$ inner-shell transition ($\lambda = 39.1$ Å) in the case of a two-step pumping for the plasma parameters $n_e = 5 \times 10^{20}$ cm^{-3}, $d = 0.1$ mm, and $T_e = 500$ eV.

An appreciable gain for a very short time ($\tau_{las} \sim 5$ ps) is possible on the short-wavelength inner-shell $3d-3p(0-1)$ transition with $\lambda = 39.1$ Å; here, the outer $4p$ electron is 'an observer,' and the transition results in a change of the vacancy in the core. This transition is of interest from the viewpoint of going to the short-wavelength range for moderate T_e. The $g(\tau)$ dependences for this transition are also given in Figs 3 and 4.

We performed calculations of $g(\tau)$ for different diameters of the plasma column d. A strong dependence on d was observed for the transition with reabsorption-induced inversion ($\lambda = 113$ Å), two more laser transitions were also found to be sensitive to the value of d. Fig. 5 shows how the gains for different transitions behave under changes of the radiating plasma diameter. For the $\lambda = 113$ Å transition, a g_{max} value is given. For a high density (Fig. 5c), the gain lowers with d for all transitions; the $\lambda = 113$ Å transition is an exception. It is noteworthy that, as the diameter d increases, the duration of 'transient' inversion for this transition increases to ~ 20 ps for the same values of parameters T_e and n_e.

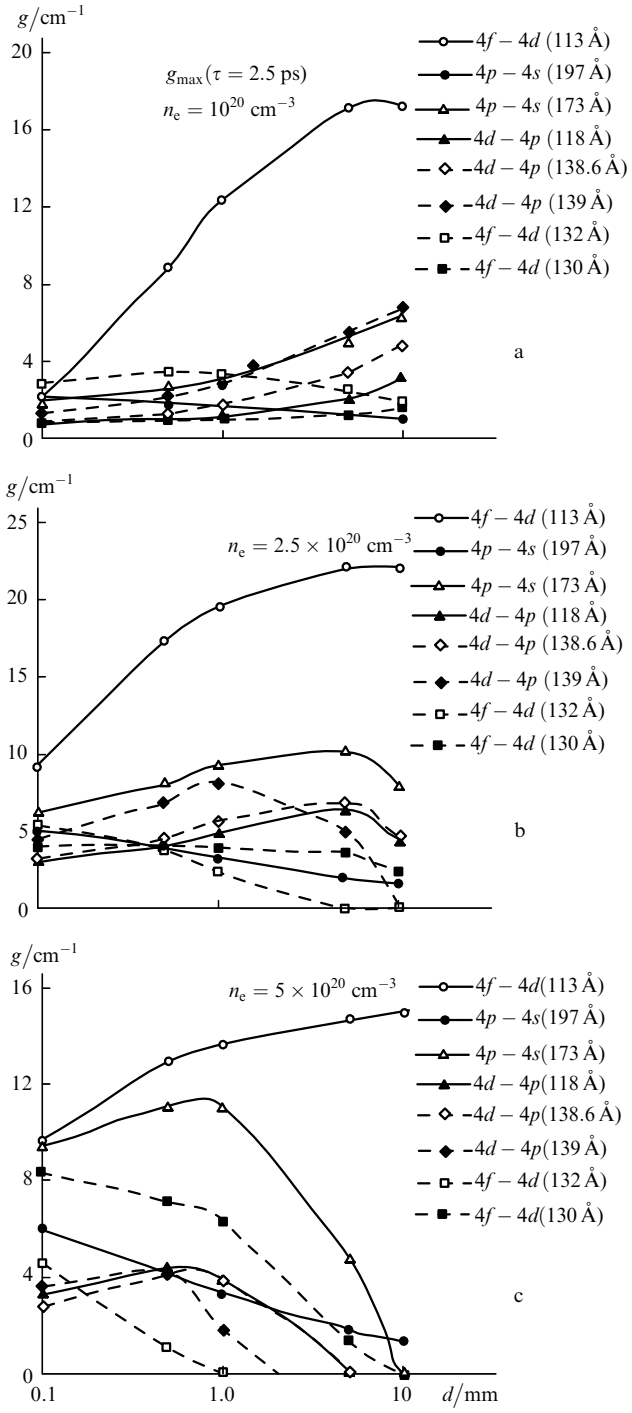

Figure 5. Dependence of the gain on the plasma diameter for $T_e = 500$ eV and different n_e; g_{max} ($\tau = 2.5$ ps) is given for the transition with reabsorption ($\lambda = 113$ Å) and the time-averaged g values for the remaining transitions.

For relatively low densities ($n_e \leqslant 3 \times 10^{20}$ cm^{-3}), the gain on the $4p - 4s(2-1)$ ($\lambda = 173$ Å), $4d - 4p(2-1)$ ($\lambda = 138.6$ Å), and $4d - 4p(3-2)$ ($\lambda = 139$ Å) transitions can be raised by increasing the plasma column diameter to several millimetres. The radiation reabsorption in the plasma was taken into account in accordance with formulas from Refs [27, 28] by invoking escape factors ε_{ij} for every transition from level i to level j: $A_{ij}^{\text{eff}} = \varepsilon_{ij} A_{ij}$, where A_{ij} is the decay probability for an isolated ion, i.e., in an optically thin medium; $\varepsilon_{ij} = 1.22[\ln(k_0 d)]^{1/2}/(k_0 d) \leqslant 1$; $k_0 \sim N_i A_{ij}$ is the photoabsorption coefficient; and N_i is the ion density. For $n_e \sim 10^{20} - 10^{21}$ cm^{-3} and $d \sim 0.1 - 5$ mm, $\varepsilon_{ij} \ll 1$ only for resonance transitions to the ground state with $\Delta J = 1$; for the remaining transitions ε_{ij} is only slightly affected. In an optically dense plasma, the population density of resonance levels rises, which may be responsible for the disappearance of inversion on transitions to the resonance state with $J = 1$. However, the population densities of the upper working levels may also rise due to collisional mixing. Accordingly, situations are in principle possible whereby the inversion is hardly dependent on the diameter or even rises with increasing diameter.

3. Conclusions

Thus, efficient ASE in Ni-like xenon is possible on the $4f - 4d(2-1)$ ($\lambda = 130$, 132 Å) and $4d - 4p(3-2)$ ($\lambda = 139$ Å) transitions for $T_e \geqslant 400$ eV, $n_e \approx 5 \times 10^{20}$ cm^{-3}. For the above plasma parameters and relatively small d, these transitions exhibit a gain–length product $gL > 50$. It is significant that gL for the conventional $4d - 4p(0-1)$ ($\lambda = 99$ Å) transition is 2–3 times lower.

The results of our calculation may be of utility in experimental investigations of the ASE in xenon plasmas [4, 6]. The commonly varied parameters are the lengths and intensities of the prepulse and the main pump pulse, and also their energy deposition ratio. Of prime importance is the selection of the time interval to record the laser line intensity. The calculation suggests that the length of the output laser pulse τ_{las} and the average value of $g(\tau)$ decrease with increase in $T_e > 600$ eV, $g_{max}(\tau)$ rising in this case. In the case of 'transient' inversion, the $g(\tau)$ function for the $4d-4p(0-1)$ transition has a sharp peak with a width ranging into the tens of picoseconds (two-step pumping). Here, the observation of amplification is possible only when the radiator is several millimetres long, the recording of only a part of the output pulse being possible for a very short radiator. It is evident that in this case, when fitting experimental intensities measured for different radiator lengths to a single-parameter model for the output beam intensity, strongly overrated g values may be obtained. This signifies that $g(\tau)$ will be different for every segment of the radiator length in the case of transient inversion. Yet another inaccuracy of $g(\tau)$ measurements may arise from the instability of the plasma filament diameter in the case of a pinching capillary discharge.

Our calculation errors are due to the uncertainties of determining the ionisation balance and also the ion temperature T_i, i.e., the Doppler component of the line width. The uncertainties of both types are eliminated by a scale factor common to all transitions for all parameter values. A more precise calculation would require an expansion of the set of simultaneous equations to calculate the kinetics of population densities, which is supposedly significant in the calculation of the gain coefficients for transitions between highly excited levels. Despite these corrections, the basic results of our work are retained.

References

1. Artyukov I A, Benvare B R, et al. *J. de Phys. IV,* **11** pt.2, 451 (2001)
2. Klisnick A, et al. *Proc. SPIE Int. Soc. Opt. Eng.* **3776** 282 (1999)

3. Lewis C L S, et al. *Proc. SPIE Int. Soc. Opt. Eng.* **3776** 292 (1999)
4. Fiedorowicz H, Bartnik A, Szczurek M, Daido H, Sakaya N, Kmetik V, Kato Y, Suzuki M, Matsumura M, Tajima J, Nakayama T, Wilhein T *Opt. Commun.* **163** 102 (1999)
5. Askar'yan G A, Tarasova N M *Pis'ma Zh. Eksp. Teor. Fiz.* **14** 89 (1971)
6. Fiedorowicz H, Bartnik A, Jarocki R, Rakowski R, Szczurek M *Appl. Phys. B* **70** 305 (2000)
7. Nickles P V, Janulewicz K A, Rocca J J, Ruhl H, Bortolotto F, Sandner W *Abstracts, VII International Conference on X-Ray Lasers* (France, 2000) p. 8
8. Molchanov A G *Usp. Fiz. Nauk* **106** 165 (1972) [*Sov. Phys. Uspekhi* **15** 124 (1972)]
9. Vinogradov A V, Sobel'man I I, Yukov E A *Kvantovaya Elektron.* **2** 105 (1975) [*Sov. J. Quantum Electron.* **5** 59 (1975)]
10. Zherikhin A N, Koshelev K N, Letokhov V S *Kvantovaya Elektron.* **3** 152 (1976) [*Sov. J. Quantum Electron.* **6** 82 (1976)]
11. MacGowan B J, Maxon S, Hagelstein P L, Keane C J, London R A, Matthews D L, Rosen M D, Scofield J H, Whelan D A *Phys. Rev. Lett.* **59** 2157 (1987)
12. MacGowan B J, Da Silva L B, Field D J, Keane C J, Koch J A, London R A, Matthews D L, Maxon S, Mrowka S, Osterheld A L, Scofield J H, Shimkaveg G, Trebes J E, Walling R S *Phys. Fluids B* **4** 2326 (1992)
13. Daido H, Kato Y, Ninomiya S, Kodama R, Yuan G, Oshikane Y, Takagi M, Takabe H *Phys. Rev. Lett.* **75** 1074 (1995)
14. Nilsen J, Moreno J C *Opt. Lett.* **20** 1387 (1995)
15. Li Y, Pretzler G, Lu P X, Fill E E *Phys. Lett. A* **53** R652 (1996)
16. Ivanova E P, Zinov'ev N A *Kvantovaya Elektron.* **27** 207 (1999) [*Quantum Electron.* **29** 484 (1999)]
17. Ivanova E P, Zinovyev N A *Phys. Lett. A* **274** 239 (2000)
18. Enright G D, Villeneuve D M, Dunn J, Baldis H A, Kieffer J C, Pepin H, Chaker M, Herman P R *J. Opt. Soc. Am.* **8** 2047 (1991)
19. Ivanova E P, Knight L V *Proc. SPIE Int. Soc. Opt. Eng.* **3776** 263 (1999)
20. Ivanov L N, Ivanova E P, Knight L V, Molchanov A G *Phys. Scr.* **53** 653 (1996)
21. Benredjem D, Sureau A, Moller C *X-Ray Lasers 1996 (Proceedings of the Fifth International Conference on X-Ray Lasers, Lund, Sweden, 1996)* S. Svanberg, C.-G. Wahlstrom (Eds) (Bristol: IOP Publishing, 1996) p. 333
22. Ivanova E P, Gulov A V *At. Data Nucl. Data Tables* **49** 1 (1991)
23. Ivanov L N, Ivanova E P, Knight L V *Phys. Rev. A* **48** 4365 (1993)
24. Ivanov L N, Ivanova E P, Knight L V *Phys. Lett. A* **206** 89 (1995)
25. Nickles P V *Phys. Rev. Lett.* **78** 2748 (1997)
26. Nilsen J, Li Y, Dunn J, Barbee T W, Osterheld A *J. de Phys.* (in press)
27. Derzhiev V I, Zhidkov A G, Yakovlenko S I *Izluchenie Ionov v Neravnovesnoi Plotnoi Plazme* (Ion Radiation in Nonequilibrium Dense Plasmas) (Moscow: Energoatomizdat, 1986)
28. Fill E *J. Quant. Spectrosc. Radiat. Transfer* **39** 489 (1988)